Dataset Dependency of Data-Driven ML Techniques in Pattern Prediction Under Mutual Coupling

Onat, N.B.; Fioranelli, F.; Yarovoy, Alexander; Aslan, Y.

DOI
10.46620/URSIATRASC24/JMTA5770

Publication date
2024

Document Version
Final published version

Published in
Proceedings of the 4th URSI Atlantic RadioScience Conference – AT-RASC 2024

4th URSI AT-RASC, Gran Canaria, 19 – 24 May 2024

Dataset Dependency of Data-Driven ML Techniques in Pattern Prediction Under Mutual Coupling

N.B. Onat, I. Roldan, F. Fioranelli, A. Yarovoy, and Y. Aslan
Delft University of Technology, Delft, the Netherlands

Abstract

This paper examines how training data affects machine learning-assisted antenna pattern prediction under mutual coupling. For demonstration, a neural network-based approach is used to predict the embedded pattern of a central patch antenna element near randomly distributed patches. It is shown that when the full-wave simulated dataset size is excessively reduced, the high prediction error in the validation set may become a critical issue. Maintaining sufficient accuracy in pattern prediction with a relatively small dataset remains an open challenge.

1 Introduction

Fast prediction of the radiation pattern of an antenna in the vicinity of other antennas or scatterers is a major challenge in array synthesis [1, 2], calibration [3], and dynamic beamforming [4, 5]. This is due to the complex effect of mutual coupling (MC), which can be determined by using full-wave simulation tools for a given topology of antennas. Despite being accurate, such an approach suffers from large computational complexity when a large number of topologies should be investigated (e.g. in case of irregular sparse array design [6]). There are effective techniques for incorporating the MC effect into the synthesis procedure [7, 8, 9]; however, the proposed methodologies tend to be either computationally expensive, tailored to specific element types, or lack the flexibility needed for application on various topologies.

In the recent years, the attention towards machine learning (ML)-based techniques has significantly grown, driven by their ability to effectively address intricate problems with notable speed and accuracy. Mainly, neural networks (NNs) are utilized on many electromagnetic (EM) problems due to their ability to approximate highly non-linear functions [10, 11]. In line with this, our previous work introduced a novel NN for efficient embedded element pattern (EEP) prediction in small planar subarrays [12].

Although the ML-based studies are promising for MC and EEP prediction, since the performance of these methodologies highly depends on the training data, it is essential to have a randomly distributed dataset with sufficient data to achieve reliable predictions while avoiding over-fitting. This study investigates how the size of dataset is crucial for the EEP prediction via NNs. Additionally, the pattern prediction performance variations in the validation set are discussed.

The rest of the paper is organized as follows. Section 2 introduces the antenna under test (AUT). Section 3 formulates the problem and presents the considered NN structure. Section 4 discusses the simulation results. The conclusions are given in Section 5.

2 Antenna Under Test (AUT)

In this study, a 5-element aperiodic array topology is considered. This comprises of a central element (the pattern of which is to be estimated) located at the origin, $(x_m, y_m) = (0,0)$, and of its neighboring elements which are randomly located with a minimum spacing of $\lambda/2$ in the region of $r^2 \leq (x_i^2 + y_i^2) \leq (2r)^2$ where (x_i, y_i) is the location of the i-th neighbor element in λ with $i = 1, ..., 4$. Furthermore, r is the radius of the defined circle that is selected as $\lambda/2$. Figure 1 illustrates the considered array topology where each element is a pin-fed patch antenna designed for the operation frequency of 2.85 GHz. The designed patch has a co-polarization electric $(e-)$ field component in θ direction, which will be referred to as the EEP.

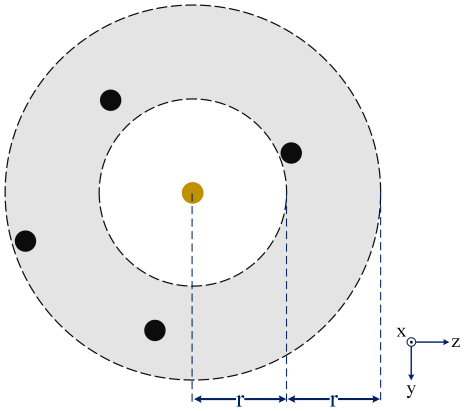

Figure 1. An example aperiodic array topology where the central element (yellow), is located at the center, and the neighboring elements (black) are randomly positioned in the defined grey region.

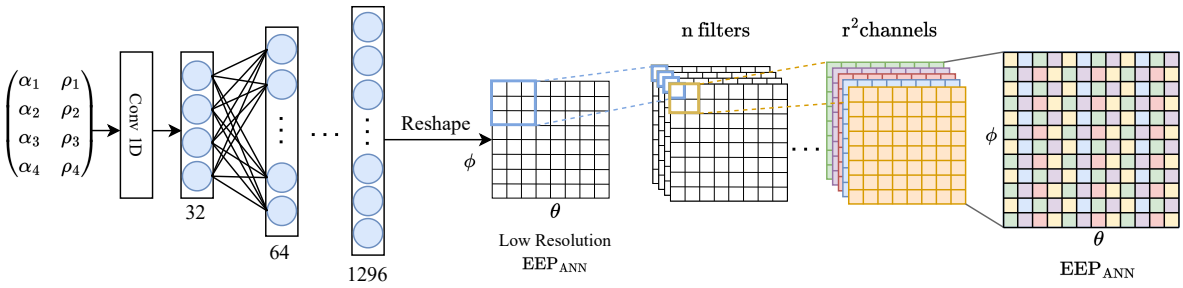

Figure 2. Block diagram of the utilized NN architecture comprising two concatenated networks based on the study in [12].

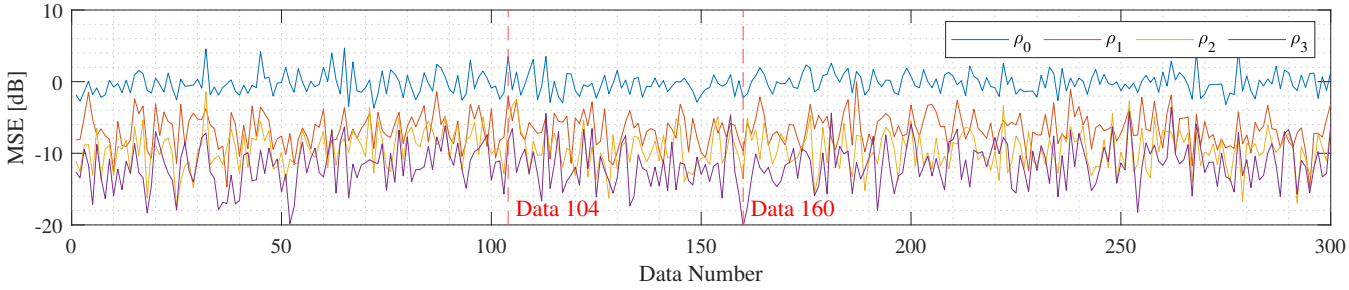

Figure 3. MSE results between the full-wave generated EEP of the full validation set and IEP (ρ_0), and predicted EEPs with the dataset sizes of 1500 (ρ_1), 2500 (ρ_2) and 3500 (ρ_3).

3 Problem Formulation and NN Architecture

Following the work in [12], this study focuses on the power pattern prediction where each EEP is a function of θ and ϕ, both having 180 samples resulting a 180×180 matrix.

The considered architecture comprises two distinct components: the initial part produces a low-resolution EEP at 36×36, and the subsequent segment scales it up to the desired resolution of 180×180, corresponding to a 1-degree resolution. The upscaling process is implemented using the efficient sub-pixel convolutional neural network (ESPCN) [13] in the upscale block as shown in Fig. 2.

Furthermore, the successful estimation of the EEP relies on utilizing the structural similarity index (SSIM) as a loss during the training of the neural network. Originally designed as a metric for evaluating image quality in the context of a reference image, typically to gauge losses from image compression, SSIM has more recently found application as a loss function in training neural networks [14].

4 Simulation Results

The effect of the dataset size and performance variation in validation set of the proposed network are discussed in this section. To this extent, 3500 simulations with random topologies were run to generate the training dataset. This size of the primary dataset is gradually decreased to 2500 and 1500 for the analysis, whereas the validation set always remains the same, comprising 300 data. The designed pin-fed patch antenna's isotropic element pattern (IEP) was simulated and compared as a benchmark. Furthermore, two extreme cases are selected for a detailed analysis.

To visualize the distribution of the datasets, polar coordinate system is used. The distance d_i for $i = 1,2,3,4$ indicates the distance (in λ) between the main the corresponding neighbor element. The angle α_{diff} is the angle between element pairs having the maximum angle separation as shown in Fig. 4a. The distance $\hat{d}$ shows the mean distance of the neighbor elements to the main element for each topology. Figure 4b illustrates the distribution of the datasets for the sizes of 1500 and 3500, where the density of the distribution increases as the data size increases. It is important to note that the angle α_{diff} remains higher then 100° due to the defined minimum element spacing of $\lambda/2$.

To quantify the prediction performance, the minimum squared error (MSE) cost function is utilized [12]:

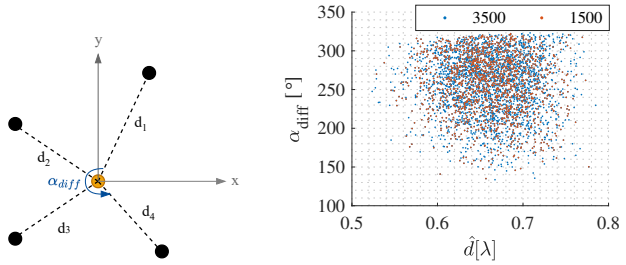

(a) Case topology **(b)** Data Distribution

Figure 4. Analysis of distribution of the training datasets.

Table 1. MSE results for the IEP, indicated with the subscript 0, and three different dataset sizes: 1500, 2500 and 3500, indicated with the subscripts 1,2 and 3, respectively.

Topology	ρ_0 **[dB]**	ρ_1 **[dB]**	ρ_2 **[dB]**	ρ_3 **[dB]**
Average	0.3	-6.06	-8.65	-10.67
Data 104	3.5	-2.05	-12.9	-15.67
Data 160	-2.23	-9.7	-13.57	-20.21

$$\rho_t = 10\lg\left(\frac{1}{N_s^2}\sum_{j,k=1}^{N_s}\left(|E_{\mathrm{CST}}(\theta_j,\phi_k)| - |E_t(\theta_j,\phi_k)|\right)^2\right) \quad (1)$$

where N_s is the total number of samples for θ and ϕ, E_{CST} is the full-wave simulated EEP of the central element generated by the commercial software CST, E_t is the predicted EEP of the same element where $t = 0,1,2,3$ indicates IEP and the sizes of the dataset 1500, 2500 and 3500, respectively.

The MSE is evaluated over the validation set and shown in Fig. 3. The error between E_{CST} and E_{IEP} (ρ_0) remains at the level of 0 dB, reaching up to 5 dB and having an average error of 0.3 dB whereas the error between E_{CST} and the prediction E_1 which is trained with the smallest dataset has an average error of -6 dB as shown in Table 1. However, the variation in the error remains high; in other words, the prediction is highly dependent on the provided dataset, where the reliability of the methodology can become questionable.

When the data size is increased to 2500, the average error is reduced by almost 3 dB, going down to nearly -9 dB. The entire dataset is used in the training, so the error scales down to almost -11 dB. Although the variations can still be observed, these variations can become negligible as the error goes down beyond -10 dB. Data 104 and 160 are analyzed as extreme cases to validate this.

Figure 5 illustrates the CST generated EEP and predicted EEPs for Data 104 which has one of the highest error rates as shown in Table 1. In this topology, the location of the elements is given as $(x_i,y_i) = \{(-0.25,-0.45),(0.2,-0.75),(0.5,0.2),(0.5,-0.3)\}$ where the neighbor elements are clustered at the top right corner, creating a special case. When the data size is low, the NN overestimates the peak region with the section

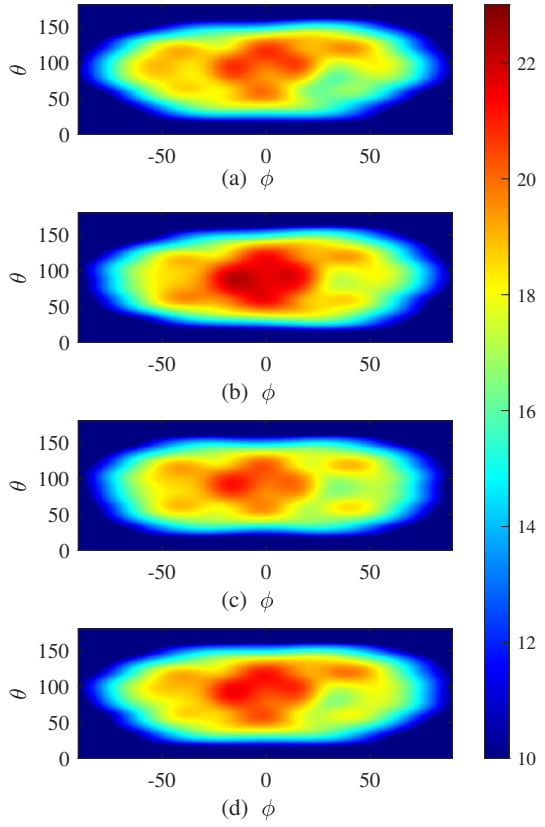

Figure 5. EEPs (e-field [dB]) for Data 104 with $(x_i,y_i) = \{(-0.25,-0.45),(0.2,-0.75),(0.5,0.2),(0.5,-0.3)\}\lambda$. (a) Full-wave simulated EEP; (b) Predicted with 1500 data; (c) Predicted with 2500 data; (d) Predicted with 3500 data.

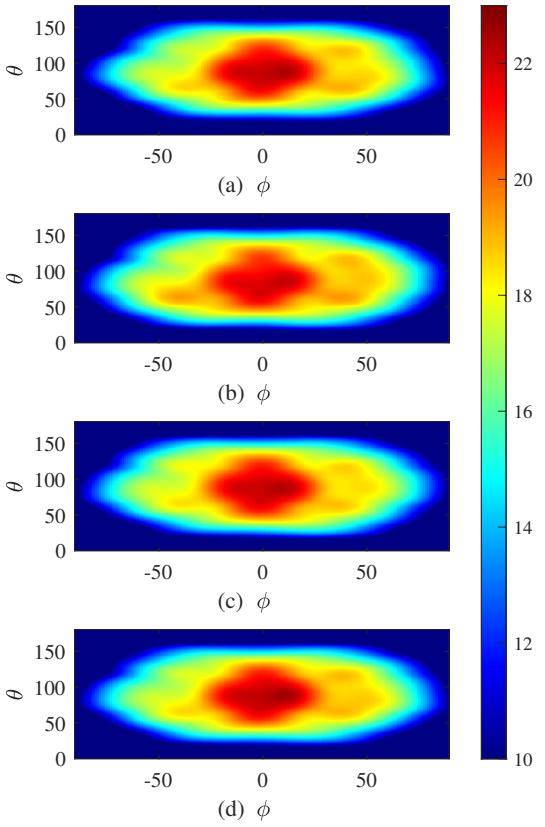

Figure 6. EEPs (e-field [dB]) for Data 160 with $(x_i,y_i) = \{(-0.6,-0.2),(0.55,0.4),(-0.25,0.65),(-0.05,-0.7)\}\lambda$. (a) Full-wave simulated EEP; (b) Predicted with 1500 data; (c) Predicted with 2500 data; (d) Predicted with 3500 data.

where $\theta < 50^\circ$ and $\phi > 0^\circ$, increasing the error rate to -2.05 dB as can be seen in Fig. 5(b). The performance of the prediction drastically increases as the data size increases, reducing the error to -15.67 dB.

On the other hand, the trained model achieves one of the best predictions in Data 160 where the elements are located at $(x_i, y_i) = \{(-0.6,-0.2),(0.55,0.4),(-0.25,0.65),(-0.05,-0.7)\}$ in λ, having an error of nearly -10 dB with the low-size and -14 dB with the 2500 data as shown in Table 1. When the entire dataset is used, the difference between the full-wave generated EEP in Fig. 6(a) and predicted EEP in Fig. 6(b) becomes almost invisible while the error rate decreases below -20 dB.

5 Conclusion

The impact of training data on ML-assisted antenna pattern prediction under mutual coupling is studied. An NN-based methodology has been used to predict the EEP of a central patch antenna element in the close vicinity of randomly-distributed patches. Two-stage networks, namely, fully connected and ESPCN, were used to achieve high-resolution. It has been shown that the performance of the network is highly dependent on the training data, where the variation of the prediction error in the validation set becomes critical with the excessive reduction in the size of the dataset. Furthermore, with the increase in the number of elements, the disturbance on the EEP by the MC effect can become a more complicated problem, reducing the reliability of the prediction with a low-size dataset. This highlights the need for developing innovative techniques to keep sufficient pattern prediction accuracy with a relatively low-size dataset.

References

[1] Tomislav Marinović et al. "Fast Characterization of Mutually Coupled Array Antennas Using Isolated Antenna Far-Field Data". In: *IEEE Transactions on Antennas and Propagation* 69.1 (2021), pp. 206–218. DOI: 10.1109/TAP.2020.3016395.

[2] Yanki Aslan, Antoine Roederer, and Alexander Yarovoy. "System Advantages of Using Large-Scale Aperiodic Array Topologies in Future mm-Wave 5G/6G Base Stations: An Interdisciplinary Look". In: *IEEE Systems Journal* 16.1 (2022), pp. 1239–1248. DOI: 10.1109/JSYST.2020.3045909.

[3] Ulf Gustavsson et al. "Implementation Challenges and Opportunities in Beyond-5G and 6G Communication". In: *IEEE Journal of Microwaves* 1.1 (2021), pp. 86–100. DOI: 10.1109/JMW.2020.3034648.

[4] Eduardo V. P. Anjos et al. "FORMAT: A Reconfigurable Tile-Based Antenna Array System for 5G and 6G Millimeter-Wave Testbeds". In: *IEEE Systems Journal* 16.3 (2022), pp. 4489–4500. DOI: 10.1109/JSYST.2022.3146360.

[5] Zhenyu Xiao et al. "A Survey on Millimeter-Wave Beamforming Enabled UAV Communications and Networking". In: *IEEE Communications Surveys Tutorials* 24.1 (2022), pp. 557–610. DOI: 10.1109/COMST.2021.3124512.

[6] J. Ignacio Echeveste et al. "Gradient-Based Aperiodic Array Synthesis of Real Arrays With Uniform Amplitude Excitation Including Mutual Coupling". In: *IEEE Transactions on Antennas and Propagation* 65.2 (2017), pp. 541–551. DOI: 10.1109/TAP.2016.2638359.

[7] J. Guzman, Miguel Aza, and Juan Zapata. "Array Pattern Synthesis of Real Antennas Using the Infinite Array Approach and Linear Programming". In: *IEEE Transactions on Antennas and Propagation* 63 (Dec. 2015), pp. 1–1. DOI: 10.1109/TAP.2015.2496106.

[8] Juan Corcoles, Jesús Rubio, and Miguel Á Gonzalez. "Spherical-Wave-Based Shaped-Beam Field Synthesis for Planar Arrays Including the Mutual Coupling Effects". In: *IEEE Transactions on Antennas and Propagation* 59.8 (2011), pp. 2872–2881. DOI: 10.1109/TAP.2011.2158950.

[9] Yanhui Liu et al. "Pattern Synthesis of Unequally Spaced Linear Arrays Including Mutual Coupling Using Iterative FFT via Virtual Active Element Pattern Expansion". In: *IEEE Transactions on Antennas and Propagation* 65.8 (2017), pp. 3950–3958. DOI: 10.1109/TAP.2017.2708081.

[10] Can Cui et al. "Synthesis of Mask-Constrained Pattern-Reconfigurable Nonuniformly Spaced Linear Arrays Using Artificial Neural Networks". In: *IEEE Transactions on Antennas and Propagation* 70.6 (2022), pp. 4355–4368. DOI: 10.1109/TAP.2022.3140214.

[11] Qi Wu et al. "Machine Learning-Assisted Array Synthesis Using Active Base Element Modeling". In: *IEEE Transactions on Antennas and Propagation* 70.7 (2022), pp. 5054–5065. DOI: 10.1109/TAP.2021.3137523.

[12] Nehir Berk Onat et al. "Efficient Embedded Element Pattern Prediction via Machine Learning: A Case Study with Planar Non-Uniform Sub-Arrays". In: *2023 17th European Conference on Antennas and Propagation (EuCAP)*. 2023, pp. 1–5. DOI: 10.23919/EuCAP57121.2023.10133770.

[13] Wenzhe Shi et al. "Real-Time Single Image and Video Super-Resolution Using an Efficient Sub-Pixel Convolutional Neural Network". In: *2016 IEEE Conference on Computer Vision and Pattern Recognition (CVPR)*. 2016, pp. 1874–1883. DOI: 10.1109/CVPR.2016.207.

[14] Hang Zhao et al. "Loss Functions for Image Restoration With Neural Networks". In: *IEEE Transactions on Computational Imaging* 3.1 (2017), pp. 47–57. DOI: 10.1109/TCI.2016.2644865.